Interlaminar toughening of resin transfer molded laminates by electrospun polycaprolactone structures: Effect of the interleave morphology

Sam van der Heijden [a], Lode Daelemans [a], Timo Meireman [a], Ives De Baere [b], Hubert Rahier [c], Wim Van Paepegem [b], Karen De Clerck [a, *]

[a] Ghent University, Department of Textiles, Technologiepark-Zwijnaarde 907, B-9052, Zwijnaarde, Belgium
[b] Ghent University, Department of Materials Science and Engineering, Technologiepark-Zwijnaarde 903, B-9052, Zwijnaarde, Belgium
[c] Vrije Universiteit Brussel, Department Materials and Chemistry, Pleinlaan 2, B-1050, Brussels, Belgium

ARTICLE INFO

ABSTRACT

Today, fiber reinforced polymer composites are a standard material in applications where a high stiffness and strength are required at minimal weight. Although fiber reinforced polymer composites show many advantages compared to other materials, delamination between reinforcing plies remains a major problem limiting further breakthrough. Previous work has shown that electrospun nanofibers can significantly improve the interlaminar fracture toughness of fiber reinforced composites thus preventing delaminations. In the present paper, the effect of the morphology of the toughening polymer is analyzed by incorporating different polycaprolactone structures in the interlaminar regions. Both Mode I and Mode II interlaminar facture toughness of composites containing five different electrospun morphologies - nanofibers, microfibers, microspheres, dense films, and PCL spray coated glass fibers - were evaluated. Analyzing the fracture behavior of the PCL toughened laminates ensures a better insight in the micromechanical fracture mechanisms behind the observed interlaminar fracture toughness and results in guidelines on the optimal interleave morphology. The results clearly demonstrate the distribution of PCL in the interlayer has a large effect on the crack path of the delamination and the resulting interlaminar fracture toughness. In order to improve the interlaminar fracture toughness in both Mode I as well as Mode II without adverse effects, porous PCL structures such as PCL nanofibers, microfibers, and microspheres are much more suitable than non-porous structures such as PCL films or spray-coated glass fibers. Among the porous structures, the nanofibers had an overall better performance with an increase in Mode I and Mode II interlaminar fracture toughness of about 60% and 80% respectively.

© 2016 Elsevier Ltd. All rights reserved.

1. Introduction

Delamination and brittle matrix fracture have long been a problem of fiber reinforced composites. They are usually due to Mode I and Mode II loading conditions of cracks which are frequently encountered during realistic loading conditions such as impact or fatigue. Recently, the use of electrospun nanofibers has been proposed to toughen composites and prevent such delaminations. A relatively diverse set of polymer nanofibers has been studied in literature for the interlaminar toughening of epoxy composites. Examples include polysulfones (PSU), poly(ether ether ketone cardo) (PEK-C), poly(ε-caprolactone) (PCL), polyamides (PA), poly(vinylidene fluoride) (PVDF), polyacrylonitrile (PAN), polyamide-imide (PAI), poly(styrene-co-glycidyl methacrylate), and polyvinyl butyral (PVB) [1–12]. Such nanofibrous nonwovens can easily be placed between two reinforcing plies prior to composite production and result in a fine distribution of the nano-scaled phases of the chosen polymer in the surrounding epoxy phase. Hence, there is no need to disperse them into the resin as opposed to traditional toughening methods, which often involve mixing reactive rubbers or thermoplastic materials in the epoxy resin (followed by phase separation during curing) [13] or the more recently applied (functionalized) nanoparticles [14–17]. This is a major advantage for infusion applications, since mixing in any

particle or thermoplastic material generally causes a large increase in viscosity.

It is well known that for thermoplastic and rubber toughening by phase separation, the final phase separated morphology of the thermoplastic/rubber phase has a major influence on the fracture toughness of the epoxy matrix [18–20]. As such also the morphology of the electrospun structure might affect the inter-laminar fracture toughness of nanofiber toughened laminates. In the present paper, we will investigate this effect by interleaving different electrospun PCL structures into resin transfer molded glass epoxy laminates to increase their fracture toughness. The study of PCL is especially relevant since some of the highest in-creases in interlaminar fracture toughness have been obtained using PCL nanofibers [6,21,22]. Both the Mode I as well as the Mode II fracture toughness of five different electrospun morphologies, i.e. nanofibers, microfibers, microspheres, films and spray coated PCL, are evaluated. Throughout this paper special emphasis will be given to analyzing the effect of the electrospun morphology on the interlaminar crack path. Since recent work by the authors showed that in a nanofiber interleaved composite laminate, the macro-scopic crack path of the delamination can be influenced by numerous parameters such as the delamination mode, the nano-fibrous veil areal density, reinforcing ply architecture, the inter-leaving method and mechanical properties of the nanofibers [23]. Hence, extensive microcopy analysis of the interlaminar crack path will provide better insight in the micromechanical fracture mech-anisms behind the observed interlaminar fracture toughness.

2. Materials and methods

2.1. Materials

All composite laminates were reinforced with unidirectional E-glass fabric with an areal density of 500 g/m^2, UDO ES500 manu-factured by SGL Group. The epoxy resin was composed of EPIKOTE resin MGS RIMR 135 with EPIKURE curing agent MGS RIMH 137 (Momentive). This is an infusion resin designed for windmill ap-plications and it has a low viscosity and a high toughness.

Polycaprolactone was supplied by scientific polymer products. The solvents 98 v% formic acid and 99.8 v% acetic acid were sup-plied by Sigma–Aldrich and used as received.

2.2. Electrospun structures

All electrospun structures where prepared on an in-house developed nozzle based electrospinning machine. The required amount of PCL was dissolved into a mixture of acetic acid (70 v%) and formic acid (30 v%). The electrospinning parameters are sum-marized in Table 1. Except for the PCL films, all of these structures were deposited directly on top of the unidirectional glass fiber fabrics and had an areal density of 5 g/m^2. The PCL films were produced using the same parameters as spray coated glass fibers, with the exception that the PCL was first electro sprayed onto aluminum foil and subsequently peeled off once all the solvent had vaporized, whereas in case of the spray coated structure, the PCL

was sprayed directly onto the unidirectional glass fiber fabrics. The PCL films had an areal density of 5 g/m^2 or 10 g/m^2 depending on whether a double or single film configuration was used.

2.3. Laminate production

The composite laminates were manufactured by vacuum assis-ted resin transfer molding (VARTM). The unidirectional glass fiber fabrics (areal density 500 g/m^2) were stacked into a steel mold in a [0°]$_8$ configuration. All glass epoxy laminates had a nominal thickness of 3 ± 0.1 mm. Electrospun PCL structures as well as an initiation film are located in the middle interlaminar region be-tween the two middle reinforcing glass fiber plies. Except for the PCL films, the electrospun structures were introduced using a double layer deposited configuration, as described in our previous work [24]. The PCL films were simply placed between the two middle glass fiber plies, where for the single film configuration the initiation film was placed on top of the PCL film and for the double PCL film configuration the initiation film was placed in between both PCL films. After infusion, the laminates were cured at room temperature for 24 h, followed by a post-cure at 80 °C for 15 h according to the manufacturer's recommended cure cycle. Although the post-curing temperature is above the melting tem-perature of PCL, our previous work has shown that the electrospun morphology of the PCL will be largely maintained after curing. After the room temperature curing step the PCL phase is already entrapped into the solid, cross-linked, epoxy network [23,25].

2.4. Tensile properties of PCL

The tensile properties of bulk PCL were measured on PCL films according to ASTM D 882. Films were used as an approximation of the properties of the PCL in the composite (after curing). It should be noted that PCL fibers might have different tensile properties due to the polymer orientation introduced by the electrospinning pro-cess [26]. However, such polymer orientations will be partially lost in the final composite since it is post-cured above the melting temperature of PCL.

2.5. Interlaminar fracture toughness

The Mode II interlaminar fracture toughness (G_{IIc}) of the lami-nates was determined by End Notched Flexure (ENF) experiments, according to a previously reported procedure [27–29]. The Mode I interlaminar fracture toughness (G_{Ic}) of the laminates was deter-mined using the Double Cantilever Beam (DCB) method according to ASTM D5528. Samples were prepared according to a previously reported procedure [9]. At least three specimens were tested for each configuration.

3. Results and discussion

3.1. Morphology and tensile properties of electrospun structures

By modifying the electrospinning parameters (section 2.1), PCL

Table 1
Electrospinning parameters used to obtain different morphologies.

	Voltage (kV)	Tip to collector distance (cm)	Flow rate (ml/h)	Substrate on collector	PCL in AA/FA mixture (wt %)
Nanofibers	24	23	2	Glass fibers	23
Microfibers	12	26	10	Glass fibers	37
Microspheres	45	34	2	Glass fibers	5
Films	11	6	2	Al Foil	5
Spray Coated	12	6	2	Glass fibers	5

nanofibers, microfibers, microspheres, spray-coated glass fibers and PCL films were produced. The nanofibers (Fig. 1A) had an average fiber diameter of 370 ± 200 nm, resulting in a highly porous structure with a very high specific surface area. This allows the nanofibrous structure to uniformly cover the complete glass fiber fabric. The microfibers (Fig. 1 B) had an average fiber diameter of 8.35 ± 0.9 μm, Due to this high fiber diameter as compared to the nanofibers, the microfiber structures have a much lower specific surface area for the same areal density. Although the microfibrous structure is also very porous, the pore size is much larger, one can clearly notice the glass fibers underneath the PCL structures. Thus the overall coverage of the microfibers was much less uniform as compared to the nanofibers. The microspheres (Fig. 1C and D) had an average diameter of 1.8 ± 0.9 μm. Although the microspheres cover the glass fibers more uniformly compared to the microfibers, the microspheres did tend to form large clusters, again resulting in regions with a varying PCL content. Finally the PCL spray-coated glassfibers and the PCL film resulted in a low porous coverage of the glassfibers (Fig. 1E and F), with the coverage of the spray-coated glassfibers being less uniform compared to the PCL film.

For a better understanding of the PCL toughening mechanisms the tensile properties of the PCL structures were compared to that of the epoxy resin (Fig. 2). PCL clearly has a much lower E-modulus and tensile strength, 195 ± 0.3 MPa and 11.3 ± 0.3 MPa as compared to 2730 ± 20 MPa and 66.1 ± 0.4 MPa for the epoxy resin [30]. The stiffness of a PCL epoxy (nano) composite is thus mainly determined by the stiffness of the epoxy. As such the volume fraction of PCL in the interlayer should not be too high as this will result in a reduction in bending stiffness of the laminate. PCL does however have a higher elongation at break ($66.7 \pm 3\%$ compared to $8.3 \pm 0.7\%$ for the epoxy) and exhibits a large amount of plastic deformation before failure. Therefore, the PCL fracture takes up significantly more energy compared to the epoxy fracture, as illustrated in Fig. 2 showing the integrated stress strain curve. This is the work required to strain the material up to a certain amount of strain. The total amount of work required to break the material is a rough approximation of its toughness. The total work of rupture is almost double for PCL as compared to the epoxy, however, the PCL has to be allowed to strain until failure ($66.7 \pm 3\%$) for this high energy uptake to occur.

3.2. Mode I fracture toughness

Fig. 3 shows the Mode I interlaminar fracture toughness values for the different configurations with, left, the porous structures (PCL nanofibers, microfibers and microspheres) and, right, the non-porous structures (PCL film, double film and spray-coated PCL). The double film has a very low Mode I interlaminar fracture toughness, whereas for a single film G_{Ic} is extremely high. The low fracture toughness of the double film configuration can be easily explained as these films hinder the infusion process. The epoxy resin is not able to penetrate through the films and as such air pockets remain present in between the two films leading to a very low interlaminar fracture toughness. SEM images of the fracture surface confirm this assumption showing only little deformation of the PCL (Fig. 4). The low toughness of the double film configuration already reveals it will be difficult to toughen more than one interlayer simultaneously since the non-porous nature of the films will prevent proper infusion of the composite, therefore limiting the practical relevance of dense non-porous PCL toughening films.

For the single PCL film interleaves the epoxy resin can flow above and below the film during infusion allowing for an air free laminate with an extremely high (nearly 100%) volume fraction of PCL in the interlayer. This PCL interlayer has a very low stiffness (section 3.1) compared to the epoxy and glass fibers surrounding it and will thus significantly influence the delamination crack path. As tension builds up at the crack tip, the relatively low modulus PCL starts to deform first. As the legs of the DCB sample are pulled further apart and the crack opening increases, extensive straining and eventual fracture through the PCL film will occur, resulting in very high G_{CI} values due to the inherent high toughness of PCL (Fig. 2). This fracture behavior is confirmed by cross sectional
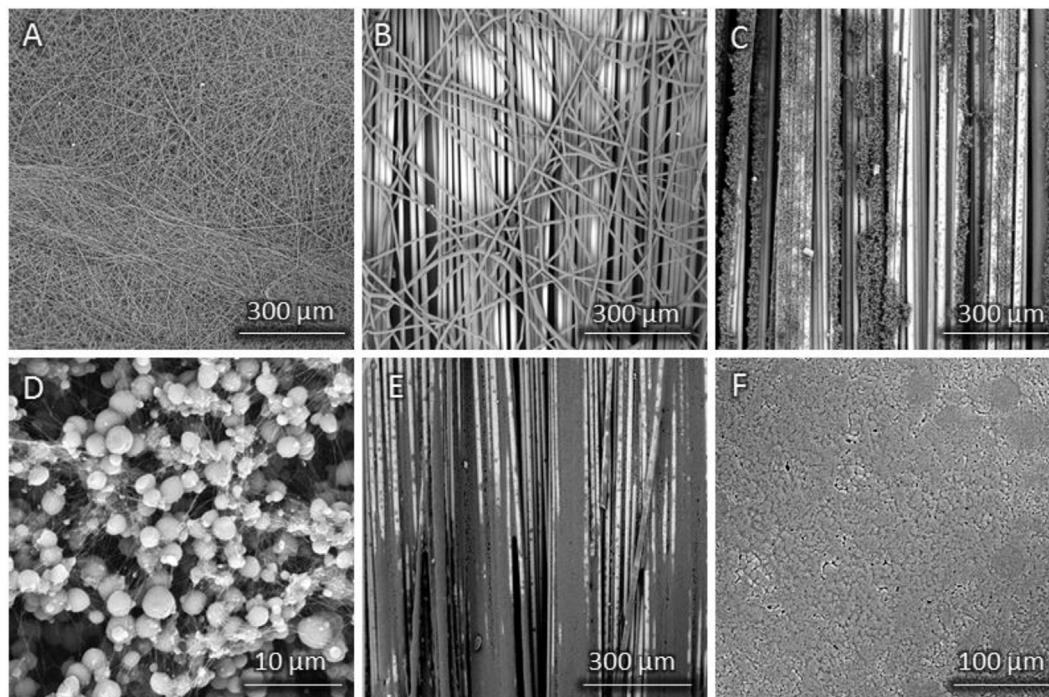

Fig. 1. SEM images of different electrospun PCL structures: A, nanofibers 370 nm; B, microfibers 8.35 μm; C and D, microspheres 1.8 μm; E, spray-coated glass fibers; F, film.
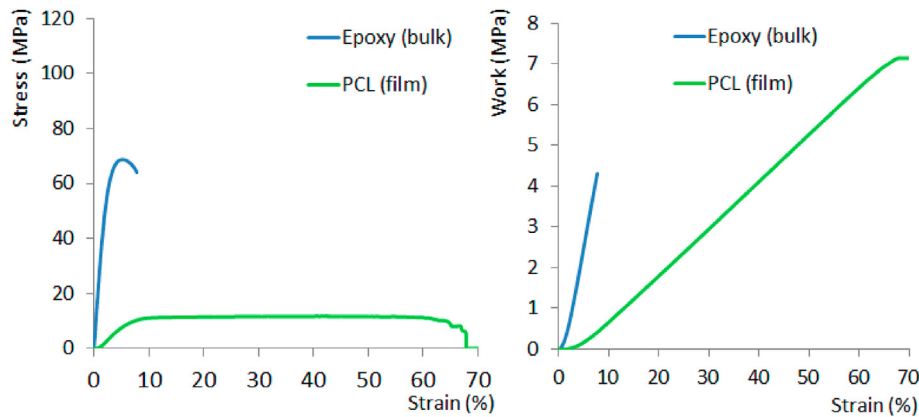
Fig. 2. Comparison of epoxy [30] and PCL tensile properties, PCL clearly has a lower stiffness and tensile strength but a higher work of rupture at larger strains.
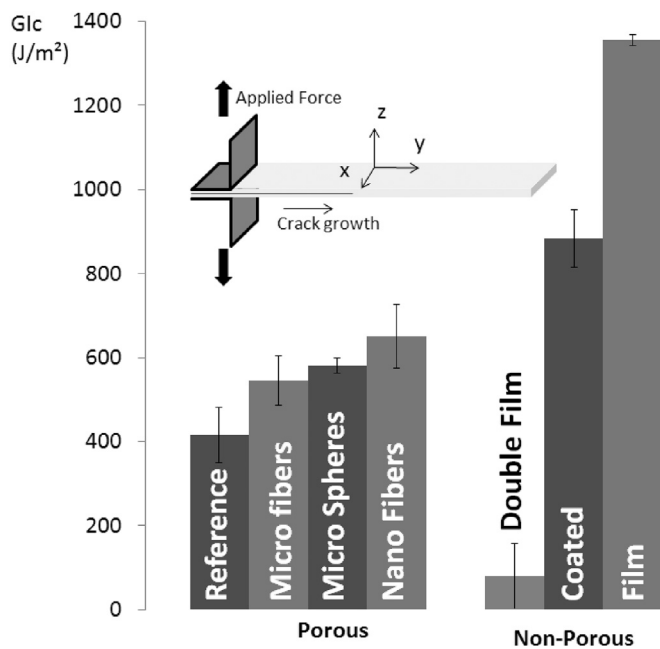

Fig. 3. Average Mode I fracture toughness values for porous structures (left) and non-porous PCL structures (right).
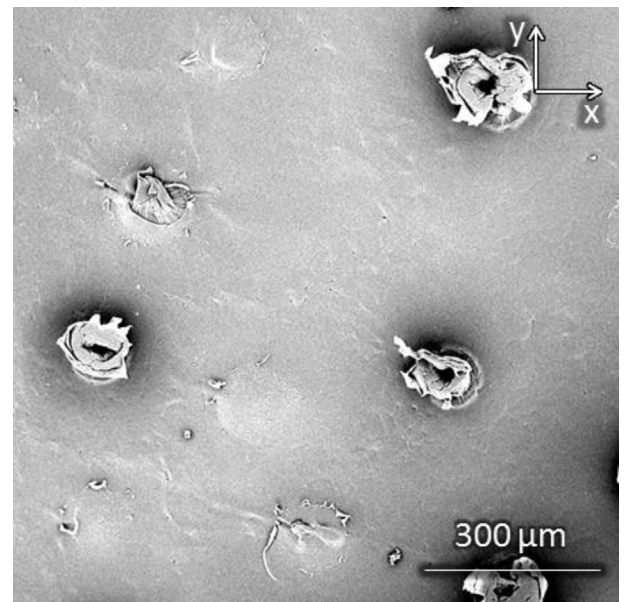

Fig. 4. SEM image of fracture surface of a DCB sample containing a double PCL film, there was little deformation of the PCL because the films hindered the infusion of epoxy resin.

images of tested DCB samples as well as SEM images from the fracture surface (Fig. 5A, see Fig. 3 for coordinate system). The microscopy images clearly show that the crack propagated directly through the PCL film, resulting in a large amount of deformed and broken PCL.

A similar fracture behavior could be observed for the laminates toughened with PCL spray-coated glass fibers (Fig. 5B) as also for these samples a low stiffness interlayer is created with a very high volume fraction of PCL thus forcing the delamination crack through the PCL interlayer. The lower performance of the PCL spray-coated glass fibers as compared to the PCL film is probably due to a less uniform distribution of the PCL or due to the presence of small air pockets between the two layers of spray-coated glass fibers since the structure has a relatively low porosity.

Although some of the Mode I results are promising for the low porous interfaces, creating such dense pure PCL interlayer(s) hinders the infusion process (by preventing through-the-thickness resin flow), thus preventing the production of laminates with multiple toughed interlayers. In addition, even if one would manage to infuse such laminates, the dense PCL interlayers will

obviously have an adverse effect on the other mechanical properties of the composite as the tensile strength and stiffness of PCL is much lower compared to epoxy (Fig. 2) and will thus reduce the shear strength, bending stiffness, creep resistance and Mode II interlaminar fracture toughness of the of the laminate (also see Section 3.3).

In contrast, the porous structures of the PCL toughened interlayer contain not only PCL, but an intense blend of small sized PCL phases and epoxy phases, thus creating an interlayer which is both relatively stiff and tough. The interlaminar crack path is also very different and one can observe both glass fiber-epoxy interfacial failure, which is typically observed for the non-toughened reference composites, as well as regular crossings of the interlaminar region through the PCL toughened interlayer (Fig. 5C—F). Both PCL and (relatively high toughness [31]), epoxy fracture will occur inside these interlaminar crossings, thus significantly more energy is required compared to a glass/epoxy interface fracture. As such the interlaminar toughness will be largely determined by the interaction of the interlaminar crack with the PCL toughened interlayer, or more specifically the amount of interlaminar crossings. This
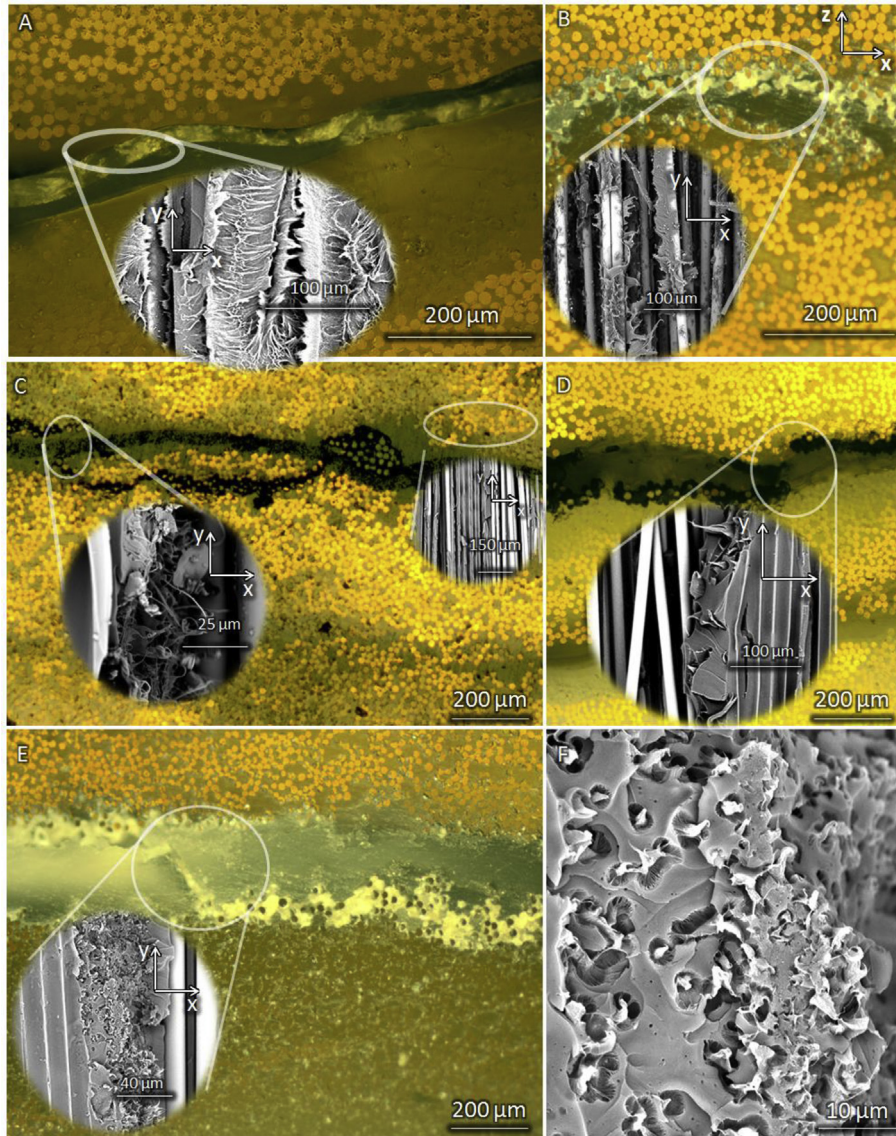
Fig. 5. Post mortem cross section of tested Mode I samples containing, A, a single film; B, spray coated glass fibers; C, PCL nanofibers; D, microfibers; E and F, microspheres. See Fig. 3 for coordinate system.

particular fracture behavior has been proposed in our previous work [32]. The present results confirm it is valid for various types of highly porous PCL morphologies, such as nanofiber structures but also microfiber and microsphere based structures.

Although the macroscopic fracture behavior of the laminates toughened with porous PCL structures was similar and the amount of PCL in the laminate was the same ($10 \, g/m^2$) for all configurations, it should be pointed out that the nanofiber structures resulted in a higher fracture toughness compared to the other porous structures. More specifically, the nanofiber toughened samples had a G_{CI} of $651 \pm 70 \, J/m^2$, an improvement of almost 60% compared to the reference composites while the microspheres and microfiber toughened samples had a G_{CI} of $580 \pm 18 \, J/m^2$ and $545 \pm 60 \, J/m^2$ respectively. These differences in Mode I interlaminar fracture toughness can be related to the fine distribution of PCL in the interlayer. For PCL nanofibers a finer distribution of nano-scaled PCL phases in the epoxy matrix can be obtained. The use of microspheres and especially microfibers resulted in a less homogeneous distribution of larger scaled PCL phases, leading to lower G_{CI} values.
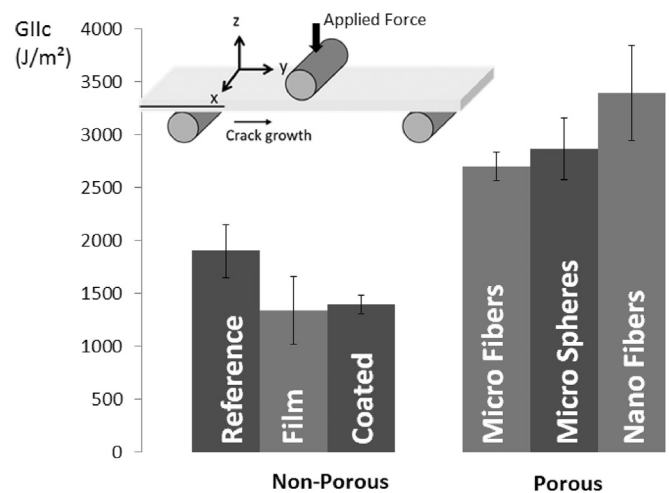

Fig. 6. Average Mode II fracture toughness values, non-porous PCL structures decrease the interlaminar fracture toughness whereas porous structures and nanofibers in particular result in a significant increase.
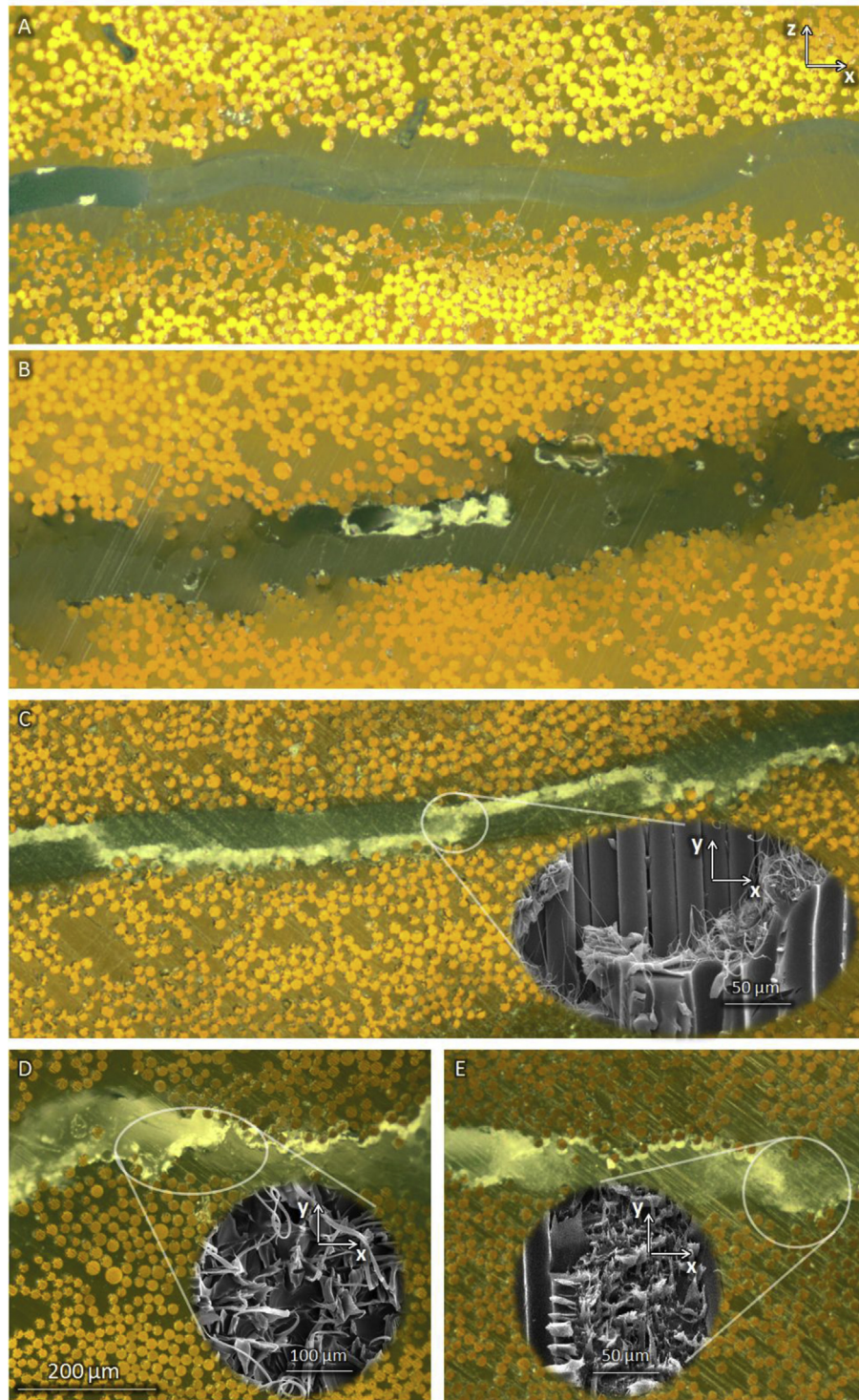
Fig. 7. Post mortem cross section of tested Mode II sample containing: A, PCL film; B, PCL spray-coated glass fibers; C, nanofibers; D, microfibers; E, microspheres. A and B show only a small amount of interlaminar cracks. In contrast C, D and E show many interlaminar crossings, resulting in a lot of deformed PCL and thus in a substantial increase in the interlaminar fracture toughness (see Fig. 3 for coordinate system).

3.3. Mode II interlaminar fracture toughness

Fig. 6 illustrates the average Mode II interlaminar fracture toughness for composites toughened with different PCL structures. The highly porous structures such as the PCL nanofibers, microfibers and microspheres significantly improve the Mode II interlaminar fracture toughness. In contrast, the non-porous structures such as the PCL film and the PCL spray coated glass fibers even have a negative effect on the Mode II interlaminar fracture toughness. The effect of porosity can again be related to the distribution of the PCL in the resin rich interlayer. As mentioned in section 3.1, the porous structures and the highly porous nanofiber

structures in particular, are completely impregnated with epoxy resin. As such the interlayer contains an intense blend of (nano-scaled) PCL and epoxy phase, resulting in an interlayer which is both stiff and tough at the same time. In contrast for a PCL film or the spray coated glass fibers, the interlayer contains a discrete layer of PCL resulting in relatively large zones of pure PCL polymer. Hence, the latter structures create an interlayer with a relatively low stiffness.

These different PCL distributions will affect how the PCL phases are strained during the Mode II delamination initiation and growth in the ENF experiment. The total strain introduced by the shear forces are distributed over the entire thickness of the interlayer. In case of the PCL film and the PCL spray-coated glass fibers, the low stiffness interlayer provides almost no resistance resulting in early stiffness reduction of the specimen. Furthermore, during the ENF test, the total relative displacement of the two sample halves remains limited and therefore the total straining in the bulk of the thick PCL interlayer (film) is limited preventing significant amounts of energy absorption (Fig. 2). Microscopic images of the cross-section perpendicular to the crack front confirm this assumption as there is very little crack growth at all (Fig. 7A–B). Furthermore, after testing it was noticed that the upper and the lower half of the composite sample containing PCL films or spray-coated glass fibers were still attached to each other, again confirming very little or no fracture occurred in the PCL film.

For the laminates toughened with porous PCL structures and PCL nanofibers in particular, the PCL zones are much smaller and are moreover fully surrounded by the epoxy resin. In addition, in line with our previous research, highlighting the importance of interlaminar crossings during crack propagation [23,25], all porous structures showed again a substantial amount of interlaminar crossings (Fig. 7C–E) resulting in a crack path through the PCL/epoxy interphase. Thus if a crack in this PCL toughened interlaminar region occurs, cracks in the epoxy matrix can be bridged by the surrounding PCL which will result in severe straining and fracture of the PCL and will take up large amounts of energy. This is only possible for the PCL morphologies that allow for a fine distribution of small sized PCL phases in the surrounding epoxy phase, thus for the highly porous morphologies. Similarly to Mode I, also the Mode II interlaminar fracture toughness of the nanofiber toughened samples is significantly higher compared to the microfiber or microsphere toughened samples. This confirms the importance of a homogeneous and very fine distribution of PCL in the interlayer.

4. Conclusions

The effect of different PCL morphologies on the Mode I and Mode II interlaminar toughness of resin transfer molded glass epoxy laminates was studied. The PCL structures are classified as non-porous (PCL films and spray-coated glass fibers) or (highly) porous structures (PCL nanofibers, microfibers and microspheres). A significant increase in the Mode II fracture toughness requires porous interleave structures. These structures have an intense fine distribution of PCL phases in a surrounding epoxy phase allowing for the PCL to strain significantly when the epoxy surrounding is cracked. The use of highly porous PCL nanofibers gave the best result. The non-porous structures could not increase the Mode II fracture toughness since they are not strained significantly during Mode II loading. As for the Mode I fracture toughness, the non-porous structures did allow for an important increase in fracture toughness. This is however combined with an expected detrimental effect on the overall mechanical properties of the composite such as the shear strength, bending stiffness and creep resistance of the laminate due to the low tensile strength and stiffness of the dense PCL interlayer. In addition the non-porous structures obstruct an

optimal infusion process and are thus not suitable. In contrast the porous structures show a more interesting Mode I fracture behavior, where interlaminar crossings of the crack path allow for an interaction with the finely distributed PCL phases in the surrounding epoxy phase, again resulting in an increased Mode I interlaminar fracture toughness. For the porous interleave structures the fine distribution and intense blend of PCL and epoxy phases ensures the overall mechanical properties of the composites.

Concluding as to improve the interlaminar fracture toughness in both Mode I as well as Mode II without adverse effects, porous PCL structures are much more suitable compared to the non-porous PCL films or spray-coated fibers, with nanofiber interleaving structures showing the best performance. The nanofiber structures allow for a straightforward method to introduce a fine distribution of the PCL phase in the epoxy matrix without the need for a complex separation process.

References

[1] J.S. Kim, D.H. Reneker, Mechanical properties of composites using ultrafine electrospun fibers, Polym. Compos. 20 (1999) 124–131, http://dx.doi.org/10.1002/pc.10340.

[2] E. Özden-Yenigün, Y.Z. Menceloğlu, M. Papila, MWCNTs/P(St-co-GMA) composite nanofibers of engineered interface chemistry for epoxy matrix nanocomposites, ACS Appl. Mater. Interfaces 4 (2012) 777–784, http://dx.doi.org/10.1021/am2014162.

[3] F. Bovicelli, H. Saghafi, T.M. Brugo, J. Belcari, A. Zucchelli, G. Minak, On consideration the mode I fracture response of CFRP composite interleaved by composite nanofibers, Procedia Mater. Sci. 3 (2014) 1316–1321, http://dx.doi.org/10.1016/j.mspro.2014.06.213.

[4] J. Zhang, T. Lin, X. Wang, Electrospun nanofibre toughened carbon/epoxy composites: effects of polyetherketone cardo (PEK-C) nanofibre diameter and interlayer thickness, Compos. Sci. Technol. 70 (2010) 1660–1666, http://dx.doi.org/10.1016/j.compscitech.2010.06.019.

[5] J. Zhang, H. Niu, J. Zhou, X. Wang, T. Lin, Synergistic effects of PEK-C/VGCNF composite nanofibres on a trifunctional epoxy resin, Compos. Sci. Technol. 71 (2011) 1060–1067, http://dx.doi.org/10.1016/j.compscitech.2011.03.008.

[6] S. van der Heijden, L. Daelemans, B. De Schoenmaker, I. De Baere, H. Rahier, W. Van Paepegem, et al., Interlaminar toughening of resin transfer moulded glass fibre epoxy laminates by polycaprolactone electrospun nanofibres, Compos. Sci. Technol. 104 (2014) 66–73, http://dx.doi.org/10.1016/j.compscitech.2014.09.005.

[7] S. Hamer, H. Leibovich, A. Green, R. Intrater, R. Avrahami, E. Zussman, et al., Mode I interlaminar fracture toughness of Nylon 66 nanofibrilmat interleaved carbon/epoxy laminates, Polym. Compos. 32 (2011) 1781–1789, http://dx.doi.org/10.1002/pc.21210.

[8] G.W. Beckermann, K.L. Pickering, Mode I and Mode II interlaminar fracture toughness of composite laminates interleaved with electrospun nanofibre veils, Compos. Part A Appl. Sci. Manuf. 72 (2015) 11–21, http://dx.doi.org/10.1016/j.compositesa.2015.01.028.

[9] B. De Schoenmaker, S. Van der Heijden, I. De Baere, W. Van Paepegem, K. De Clerck, Effect of electrospun polyamide 6 nanofibres on the mechanical properties of a glass fibre/epoxy composite, Polym. Test. 32 (2013) 1495–1501, http://dx.doi.org/10.1016/j.polymertesting.2013.09.015.

[10] R. Palazzetti, A. Zucchelli, C. Gualandi, M.L. Focarete, L. Donati, G. Minak, et al., Influence of electrospun Nylon 6,6 nanofibrous mats on the interlaminar properties of Gr–epoxy composite laminates, Compos. Struct. 94 (2012) 571–579, http://dx.doi.org/10.1016/j.compstruct.2011.08.019.

[11] K. Bilge, S. Venkataraman, Y.Z. Menceloglu, M. Papila, Global and local nanofibrous interlayer toughened composites for higher in-plane strength, Compos. Part A Appl. Sci. Manuf. 58 (2014) 73–76.

[12] G. Li, P. Li, C. Zhang, Y. Yu, H. Liu, S. Zhang, et al., Inhomogeneous toughening of carbon fiber/epoxy composite using electrospun polysulfone nanofibrous membranes by in situ phase separation, Compos. Sci. Technol. 68 (2008) 987–994, http://dx.doi.org/10.1016/j.compscitech.2007.07.010.

[13] W.D. Bascom, D.L. Hunston, Rubber-toughened Plastics, vol. 222, American Chemical Society, Washington, DC, 1989, http://dx.doi.org/10.1021/ba-1989-0222.

[14] J.M. González-Domínguez, A. Ansón-Casaos, A.M. Díez-Pascual, B. Ashrafi, M. Naffakh, D. Backman, et al., Solvent-free preparation of high-toughness

epoxy-SWNT composite materials, ACS Appl. Mater. Interfaces 3 (2011) 1441—1450, http://dx.doi.org/10.1021/am101260a.

[15] W. Yu, J. Fu, X. Dong, L. Chen, H. Jia, L. Shi, Highly populated and nearly monodispersed nanosilica particles in an organic medium and their epoxy nanocomposites, ACS Appl. Mater. Interfaces 5 (2013) 8897—8906, http://dx.doi.org/10.1021/am402845d.

[16] Y. Martinez-Rubi, B. Ashrafi, J. Guan, C. Kingston, A. Johnston, B. Simard, et al., Toughening of epoxy matrices with reduced single-walled carbon nanotubes, ACS Appl. Mater. Interfaces 3 (2011) 2309—2317, http://dx.doi.org/10.1021/am200523z.

[17] L. Chen, S. Chai, K. Liu, N. Ning, J. Gao, Q. Liu, et al., Enhanced epoxy/silica composites mechanical properties by introducing graphene oxide to the interface, ACS Appl. Mater. Interfaces 4 (2012) 4398—4404, http://dx.doi.org/10.1021/am3010576.

[18] J.H. Hodgkin, G.P. Simon, R.J. Varley, Thermoplastic toughening of epoxy resins: a critical review, Polym. Adv. Technol. 9 (1998) 3—10, http://dx.doi.org/10.1002/(SICI)1099-1581(199801)9:1<3::AID-PAT727>3.0.CO;2-I.

[19] R.J. Varley, J.H. Hodgkin, Effect of reinforcing fibres on the morphology of a toughened epoxy/amine system, Polym. Guildf. 38 (1997) 1005—1009, http://dx.doi.org/10.1016/S0032-3861(96)00596-4.

[20] A.J. MacKinnon, S.D. Jenkins, P.T. McGrail, R.A. Pethrick, A dielectric, mechanical, rheological and electron microscopy study of cure and properties of a thermoplastic-modified epoxy resin, Macromolecules 25 (1992) 3492—3499, http://dx.doi.org/10.1021/ma00039a029.

[21] G. Li, P. Li, C. Zhang, Y. Yu, H. Liu, S. Zhang, et al., Inhomogeneous toughening of carbon fiber/epoxy composite using electrospun polysulfone nanofibrous membranes by in situ phase separation, Compos. Sci. Technol. 68 (2008) 987—994, http://dx.doi.org/10.1016/j.compscitech.2007.07.010.

[22] H. Saghafi, A. Zucchelli, R. Palazzetti, G. Minak, The effect of interleaved composite nanofibrous mats on delamination behavior of polymeric composite materials, Compos. Struct. 109 (2014) 41—47, http://dx.doi.org/10.1016/j.compstruct.2013.10.039.

[23] L. Daelemans, S. van der Heijden, I. De Baere, H. Rahier, W. Van Paepegem, K. De Clerck, Damage resistant composites using electrospun nanofibers: a multiscale analysis of the toughening mechanisms, ACS Appl. Mater. Interfaces 8 (2016) 11806—11818, http://dx.doi.org/10.1021/acsami.6b02247.

[24] S. van der Heijden, L. Daelemans, B. De Schoenmaker, I. De Baere, H. Rahier, W. Van Paepegem, et al., Interlaminar toughening of resin transfer moulded glass fibre epoxy laminates by polycaprolactone electrospun nanofibres, Compos. Sci. Technol. 104 (2014) 66—73, http://dx.doi.org/10.1016/j.compscitech.2014.09.005.

[25] S. van der Heijden, L. Daelemans, B. De Schoenmaker, I. De Baere, H. Rahier, W. Van Paepegem, et al., Interlaminar toughening of resin transfer moulded glass fibre epoxy laminates by polycaprolactone electrospun nanofibres, Compos. Sci. Technol. 104 (2014) 66—73, http://dx.doi.org/10.1016/j.compscitech.2014.09.005.

[26] E.P.S. Tan, S.Y. Ng, C.T. Lim, Tensile testing of single ultrafine polymeric fiber, Biomaterials 26 (2005) 1453—1456.

[27] L. Daelemans, S. van der Heijden, I. De Baere, H. Rahier, W. Van Paepegem, K. De Clerck, Nanofibre bridging as a toughening mechanism in carbon/epoxy composite laminates interleaved with electrospun polyamide nanofibrous veils, Compos. Sci. Technol. 117 (2015) 244—256, http://dx.doi.org/10.1016/j.compscitech.2015.06.021.

[28] I. De Baere, S. Jacques, W. Van Paepegem, J. Degrieck, Study of the mode i and mode II interlaminar behaviour of a carbon fabric reinforced thermoplastic, Polym. Test. 31 (2012) 322—332, http://dx.doi.org/10.1016/j.polymertesting.2011.12.009.

[29] A. Arrese, N. Carbajal, G. Vargas, F. Mujika, A new method for determining mode II R-curve by the End-Notched Flexure test, Eng. Fract. Mech. 77 (2010) 51—70, http://dx.doi.org/10.1016/j.engfracmech.2009.09.008.

[30] K. Allaer, I. De Baere, P. Lava, W. Van Paepegem, J. Degrieck, On the in-plane mechanical properties of stainless steel fibre reinforced ductile composites, Compos. Sci. Technol. 100 (2014) 34—43, http://dx.doi.org/10.1016/j.compscitech.2014.05.009.

[31] L. Daelemans, S. van der Heijden, I. De Baere, I. Muhammad, W. Van Paepegem, H. Rahier, et al., Bisphenol A based polyester binder as an effective interlaminar toughener, Compos. Part B Eng. 80 (2015) 145—153, http://dx.doi.org/10.1016/j.compositesb.2015.05.044.

[32] L. Daelemans, S. van der Heijden, I. De Baere, H. Rahier, W. Van Paepegem, K. De Clerck, Damage-resistant composites using electrospun nanofibers: a multiscale analysis of the toughening mechanisms, ACS Appl. Mater. Interfaces 8 (2016) 11806—11818, http://dx.doi.org/10.1021/acsami.6b02247.